HHS Public Access

Author manuscript

Eur J Neurosci. Author manuscript; available in PMC 2019 June 24.

Published in final edited form as:

Eur J Neurosci. 2019 January ; 49(1): 27–39. doi:10.1111/ejn.14223.

Inhibition of calcium/calmodulin-dependent protein kinase kinase (CaMKK) exacerbates impairment of endothelial cell and blood–brain barrier after stroke

Ping Sun, **Fan Bu**, **Jia-Wei Min**, **Yashasvee Munshi**, **Matthew D. Howe**, **Lin Liu**, **Edward C. Koellhoffer**, **Li Qi**, **Louise D. McCullough**, and **Jun Li**

Department of Neurology, McGovern Medical School, University of Texas Health Science Center at Houston, Houston, Texas

Abstract

Brain microvascular endothelial cells play an essential role in maintaining blood–brain barrier (BBB) integrity, and disruption of the BBB aggravates the ischemic injury. CaMKK (α and β) is a major kinase activated by elevated intracellular calcium. Previously, we demonstrated that inhibition of CaMKK exacerbated outcomes, conversely, overex-pression reduced brain injury after stroke in mice. Interestingly, CaMKK has been shown to activate a key endothelial protector, sirtuin 1 (SIRT1). We hypothesized that CaMKK protects brain endothelial cells via SIRT1 activation after stroke. In this study, Oxygen-Glucose Deprivation (OGD) was performed in human brain microvascular endothelial cells. Stroke was induced by middle cerebral artery occlusion (MCAO) in male mice. Knockdown of CaMKK β using siRNA increased cell death following OGD. Inhibition of CaMKK β by STO-609 significantly and selectively down-regulated levels of phos-phorylated SIRT1 after OGD. Changes in the downstream targets of SIRT1 were observed following STO-609 treatment. The effect of STO-609 on cell viability after OGD was absent, when SIRT1 was concurrently inhibited. We also demonstrated that STO-609 increased endothelial expression of the proinflammatory proteins ICAM-1 and VCAM-1 and inhibition of CaMKK exacerbated OGD-induced leukocyte-endothelial adhesion. Finally, intracerebroventricular injection of STO-609 exacerbated endothelial apoptosis and reduced BBB integrity after 24-hr reperfusion following MCAO in vivo. Collectively, these results demonstrated that CaMKK inhibition reduced endothelial cell viability, exacerbated inflammatory responses and aggravated BBB impairment after is-chemia. CaMKK activation may attenuate ischemic brain injury via protection of the microvascular system and a reduction in the infiltration of pro-inflammatory factors.

Correspondence: Jun Li, Department of Neurology, McGovern Medical School, University of Texas Health Science Center at Houston, Houston, TX. jun.li.3@uth.tmc.edu.

AUTHOR CONTRIBUTIONS

Ping Sun performed the majority of the experiments; Fan Bu, Matthew D. Howe, Jia-wei Min and Yashasvee Munshi performed parts of the experiments; Lin Liu, Edward C. Koellhoffer and Li Qi provided technical supports; Jun Li designed experiment; Jun Li and Louise D. McCullough supervised the experiments; Ping Sun and Jun Li are responsible for writing and editing the manuscript.

CONFLICT OF INTEREST

The authors declare that there is no conflict of interest.

DATA ACCESSIBILITY

All data are provided in full in the results section of this paper. The authors confirm that all data underlying the finding are available and will be shared with the research community upon request.

Keywords

blood-brain barrier; calcium/calmodulin-dependent protein kinase kinase; endothelial cells; sirtuin 1; stroke

1 | INTRODUCTION

Endothelial cells are major components of the blood–brain barrier (BBB) and play an important role in BBB function via the development of a highly selective barrier (Pan et al., 2016). Cerebral ischemia results in injury or death of cerebral endothelial cells, which is well known to lead to poorer clinical outcomes in stroke patients. Mounting evidence has shown that ischemia-induced cerebral endothelial injury or death increases vascular permeability and BBB disruption (Sandoval & Witt, 2008; Yin et al., 2010). It is well known that increased vascular permeability promotes hemorrhagic transformation and edema formation, which are major contributors to mortality in stroke patients. In addition, endothelial injury increases the infiltration of peripheral proinflammatory leukocytes, including T cells, B cells and neutrophils, and the release of proinflammatory mediators. Impairment of endothelial cells results in increased secretion of pro-inflammatory cytokines (Sandoval & Witt, 2008). Therefore, understanding the mechanisms of cerebral endothelium injury in stroke is very important for the development of therapeutic treatments.

The serine/threonine-specific protein kinase CaMKK is a major kinase activated by elevated intracellular calcium. Evidence suggests that CaMKK may act as an endogenous protector of endothelial cells after stroke. Intracellular calcium/calmodulin signaling directly activates CaMKK, which exists as two isoforms, α and β. Activated CaMKK phosphorylates its two primary downstream targets, CaMK I and CaMK IV (McCullough et al., 2013). We have previously demonstrated that CaMKK is neuroprotective in stroke. Our previous data demonstrated that CaMKK signaling reduced ischemic injury because pharmacological inhibition of CaMKK by STO-609 exacerbated ischemic damage (McCullough et al., 2013), conversely, overexpression reduced brain injury in mice (Liu et al., 2016). Interestingly, we demonstrated that CaMKK β and CaMK IV KO mice exhibited increased hemorrhagic transformation rates and activation of matrix metalloproteinases, which suggested that CaMKK may be an endogenous protectant of the BBB in stroke. Moreover, CaMKK has been shown to activate a key endothelial protector, sirtuin 1 (SIRT1), but the interaction between these two proteins has not been examined in stroke. We hypothesized that CaMKK protects brain endothelial cells (ECs) via SIRT1 activation after stroke. This study used in vitro and in vivo models of stroke to investigate the role of CaMKK signaling in the impairment of endothelial cells and BBB after stroke and further examined the underlying molecular mechanisms.

2 | MATERIAL AND METHODS

2.1 | Cell culture and transfection

Human brain microvascular endothelial cells (HBEC-5i) were purchased from American Type Culture Collection (ATCC, VA, USA). These cells were isolated from male donors.

HBEC-5i cells were cultured as recommended on 0.1% gelatin (EMD Millipore)-coated plates in DMEM/F12 (Thermo-Fischer Scientific) supplemented with 10% FBS (fetal bovine serum, Life Technologies) and 40 μg/ml endothelial growth supplement (ECGS, Thermo-Fisher Scientific). THP-1 monocytic cells were obtained from American Type Culture Collection (ATCC, VA, USA) and grown in RPMI 1640 medium (Thermo-Fisher Scientific) supplemented with 10% FBS and 0.05 mM 2-mercaptoethanol. For cell viability and adhesion assays, HBEC-5i cells were seeded at 50,000/ml and grown for 48 hr to reach 80%–90% confluence before treatment. For immunoblot analyses, cells were seeded at 60,000/ml and grown to 80%–90% confluence before treatment. All cells were maintained at 37°C in a humidified atmosphere containing 5% CO_2.

HBEC-5i cells were transfected with CaMKK β siRNA (Santa Cruz Biotechnology) to knock down CaMKK β ex-pression. Briefly, HBEC-5i cells in six-well tissue culture plates were transfected with 60 nM CaMKK β siRNA or 60 nM control siRNA in the presence of siRNA transfection reagent and transfection medium for 7 hr at 37°C in a 5% CO_2 incubator when the cells were 60%–80% confluent. One milliliter of normal growth medium containing 2× normal serum and antibiotic concentration was added and cells were incubated for an additional 24 hr, followed by aspiration of the medium and replacement with fresh 1× normal growth medium for 24 hr prior to oxygen and glucose deprivation (OGD) and reoxygen-ation treatments.

2.2 | OGD model and cell treatment

Combined OGD and reoxygenation were performed as an “in vitro” experimental approach to ischemic stroke, as previously described (Sun et al., 2015) with modifications. For OGD treatment, HBEC-5i endothelial cells were washed with glucose-free PBS, incubated in glucose-free DMEM (Thermo-Fisher Scientific), and placed in a hypoxic cham-ber (model MIC-101, Billups-Rothenberg). Hypoxic environments were achieved by flushing the chamber for 10 min with 5% CO_2-balanced N_2. The hypoxia chamber was then transferred to a 37°C incubator. Control cells were maintained in DMEM (5 mM glucose) in the incubator under normoxic conditions (5% CO_2/95% air). For reoxygenation, we added 5 mM glucose to cells subjected to OGD, which returned the cells to normoxic conditions.

For cell viability and adhesion assays, HBEC-5i cells were seeded at 25,000 cells/well (24-well plate) and grown for 72 hr to reach 80%–90% confluence before treatments. For immunoblot analysis, cells were seeded at 300,000 cells/dish (60-mm diameter) and grown for 48 hr to reach 80%–90% confluence prior to treatments. DMSO (dimethylsulfoxide, 0.1%), STO-609 (10 μM) and EX-527 (2 μM) were added to DMEM before the OGD. Compounds in the reoxygenation process were maintained at the same concentrations as during the OGD.

2.3 | Animals

The study was performed in accordance with the NIH Guidelines for the Care and Use of Laboratory Animals. All protocols were approved by the Center for Laboratory Animal Medicine and Care at the Medical School of University of Texas Health Science Center in

Houston. Male (20–25 g) C57BL/6J wild-type mice were purchased from Jackson Laboratory.

2.4 | Mouse model of middle cerebral artery occlusion

Focal transient cerebral ischemia was induced via 90 min of middle cerebral artery occlusion followed by reperfusion, as described previously (Liu et al., 2014; McCullough et al., 2013; Yuan et al., 2016). Briefly, mice were anesthetized initially with 4% isoflurane, and 1.5% isoflurane was used for maintenance. The common carotid artery (CCA), external carotid artery (ECA) and internal carotid artery (ICA) were isolated. A silicon-coated monofilament suture (filament size 6–0) was inserted into the ICA via an ECA stump, and the suture was gently advanced to block MCA blood flow. For reperfusion, the mice were reanesthetized and the suture was carefully withdrawn 90 min after the occlusion. Mice in sham group underwent the same procedures without MCA occlusion. Animals were randomized into stroke and sham cohorts, the investigators who performed the procedures were blinded to drug treatment.

For postsurgery care, postsurgical animals were kept on temperature-controlled warming pad for 4 hr after surgery. Sterile 0.9% NaCl solution was injected subcutaneously after the surgery if blood loss or dehydration was suspected (0.5 ml mouse^{-1} day^{-1}) depending on the mouse health status. Animals were monitored until sternal recumbency was reached before the animals were returned to the animal facility. Moistened mashed rodent chow and water were provided on the floor of the cages.

2.5 | Drug treatment in mice

The CaMKK β inhibitor STO-609 was prepared and injected as described previously (McCullough et al., 2013). Briefly, STO-609 was dissolved in DMSO at 1.5 mg/ml, and 2 μl of the STO-609 solution was injected intracerebroventricularly in male WT mice 1 hr prior to the onset of middle cerebral artery occlusion at the following coordinates from bregma: −0.9 mm lateral, −0.1 mm posterior, −3.1 mm depth. Control animals were injected with equal amounts of vehicle (DMSO).

2.6 | Quantitation of Evans blue extravasation

Cerebrovascular permeability analyses were performed as previously described (Manaenko, Chen, Kammer, Zhang, & Tang, 2011; Yin et al., 2013) with modifications. Briefly, 23 hr after a 90-min period of MCAO, mice were injected with 100 μl of 4% Evans blue (Sigma-Aldrich) via the right femoral vein. One hour later, the mice were anesthetized by intraperitoneal injection of tribromoethanol (Avertin®) at a dose of 0.25 mg/g of body weight, and then transcardially perfused with 0.1 M sodium phosphate buffer (pH 7.4) to clear the blood and EB remaining in the vascular system, and the brains were removed quickly. Each hemisphere was weighed, homogenized in *N,N*-dimethylformamide and centrifuged at 25,000 *g* for 45 min. The supernatants were collected, and Evans blue extravasation in each hemisphere was quantitated using the following formula: $\{A_{620}\text{ nm} - [(A_{500}\text{ nm} + A_{740}\text{ nm})/2]\}$/mg wet weight. Background Evans blue levels in the non-ischemic hemisphere were subtracted from the ischemic hemisphere ipsilateral to the MCAO (Yin et al., 2010). For endothelial cell apoptosis assays, mice were perfused by PBS and then

PFA (4%) 24 hr after MCAO. Brains were sliced and stained for endothelial cells and apoptosis. We used antibody for CD31 at 1:200 (#550274, BD Biosciences) and secondary antibody at 1:500 (#A11006, Life technologies, Alexa Fluor 488) for detecting endothelial cells. For detecting early apoptosis, we used cleaved Caspase-3 antibody at 1:500 (#559565, BD Biosciences) and secondary antibody at 1:500 (#A11072, Thermo Fisher SCIENTIFIC, Alexa Fluor 594).

2.7 | Cell viability assay

The MTT [3-(4,5-dimethylthiazol-2-yl)-2,5-diphenyltetrazol ium bromide] reduction method was used to evaluate cell viability. Briefly, cells were incubated in 0.5 mg/ml MTT for 1.5 hr at 37°C after treatment. The medium was then replaced with DMSO to dissolve the blue formazan precipitate, which was spectrophotometrically quantitated at 560 and 620 nm in a multimode plate reader (PerkinElmer; Plumb, Milroy, & Kaye, 1989).

Quantitation of cell viability was also assessed using a CCK-8 cell counting kit (Dojindo, ck04–05; Okada & Okada, 2013; Yuan et al., 2016) according to the manufacturer's instruction. Briefly, cells were incubated with a CCK-8 solution (1:10 to medium volume per well) containing medium at the end of each treatment for 2 hr at 37°C. Absorbance at 450 nm was measured using a multimode plate reader (PerkinElmer).

2.8 | Western blot analysis

Cells were collected in 1× RIPA buffer containing 1 mM PMSF and sonicated for 10 s. Protein concentrations were measured using the bicinchoninic acid (BCA) assay (Pierce). Equal amounts of protein (20 μg/lane) were loaded onto 4%–15% precast protein gels (Bio-Rad) and transferred to polyvinylidene difluoride (PVDF, Bio-Rad) membranes. Membranes were blocked for 1 hr with TBS/0.1%-Tween buffer plus 5% (w/v) non-fat dried milk and incubated overnight at 4°C with primary antibodies dissolved in blocking buffer. Membranes were incu-bated with secondary antibodies for 1 hr and developed using a Pierce® ECL Western blotting detection kit (Thermo Scientific) and a ChemiDoc XRS System (Bio-Rad). Image lab software was used to quantitate Western blot signals. The following primary antibodies were used in this study: mouse anti-CaMKK β (1:200; Santa Cruz Biotechnology), rabbit anti-SIRT1 (1:1000; Cell Signaling), rabbit anti-phospho-SIRT1 (1:1000; Cell Signaling), rabbit anti-phospho-CAMKIV (1:1000; Abcam), rabbit anti-eNOS (1:1000; Cell Signaling), rabbit anti-VCAM-1 (1:1000; Cell Signaling), rabbit anti-CD54/ICAM1 (1:1000;Cell Signaling) and mouse anti-β-actin (1:5000; Sigma-Aldrich). HRP (horseradish peroxidase)-conjugated anti-rabbit IgG (1:2000; Vector Laboratories) and HRP-conjugated anti-mouse IgG (1:2000; Vector Laboratories) were used as secondary antibodies.

2.9 | Adhesion assay

Leukocyte-endothelial cell adhesion assays were performed as described previously (Sun, Sole, & Unzeta, 2014; Sun et al., 2015, 2018). Briefly, 40 min before the end of the treatments, THP-1 monocytes were labeled with 1 μM cal-cein AM in FBS-free RPMI 1640 medium, and endothelial cells were incubated with calcein AM-labeled THP-1 monocytes (2.5×10^5 per well in 24-well plates) for 40 min at 37°C. Unbound monocytes were

removed by carefully washing the plates at least three times with FBS-free RPMI 1640 medium. The fluorescence intensity was measured using a fluorescence multimode plate reader ($\lambda_{ex}/\lambda_{em}$: 495/530 nm, PerkinElmer). The results are presented as the percentage of fluorescence intensity of treated cells to control cells.

2.10 | Statistical analysis

The results are given as the means ± *SEM* of independent experiments. Differences among three or more groups were statistically analyzed by ANOVA and Holm-Sidak multiple comparison test. $p < 0.05$ was considered statistically significant. Statistical analyses and graphic representations were obtained using Graph-Pad Prism 6.0 software.

3 | RESULTS

3.1 | Pharmacological CaMKK β inhibition with STO-609 aggravated cell damage in OGD with reoxygenation conditions

Different concentrations (1.0–10 μM) of STO-609 were incubated with HBEC-5i endothelial cells under normoxic conditions, compared with control, no influences on cell viability were observed with 1.0–10 μM STO-609 treatments (Figure 1a). The dose response of STO-609 under control conditions was done to select doses of STO-609 for further experiments under OGD. We selected a range of potentially effective doses of STO-609, based on its EC50 value, and tested them for cytotoxicity under normoxia conditions. Ten micrometre of STO-609, the highest dose that displayed no cytotoxicity in control condition, was chosen to investigate the role of CaMKK β under OGD conditions as it may provide most robust inhibition. HBEC-5i endothelial cells treated with 10 μM STO-609 were subjected to OGD with reoxygen-ation conditions. Statistical analysis using One-Way ANOVA found significant main effects in both CCK-8 cell viability assays ($F_{5,21} = 23.81$, $p < 0.0001$; Figure 1b) and MTT reduction assay ($F_{5,26} = 14.99$, $p < 0.0001$; Figure 1b). Multiple comparisons post hoc analyses revealed that 18 hr-OGD with 24-hr reoxygenation of HBEC-5i cells induced approximately 30% cell death in CCK-8 cell viability assays ($p_{adj} = 0.0017$; Figure 1b) and approximately 25% cell death in the MTT reduction assay ($p_{adj} = 0.0031$; Figure 1c) compared with each Ctrl. STO-609 treatment of HBEC-5i endothelial cells ex-acerbated cell death compared with vehicle (DMSO, 0.1%) treatment after 18-hr OGD with 24-hr reoxygenation in the CCK-8 cell viability assay (cell viability: DMSO 66.50 ± 4.74 vs. STO-609 51.82 ± 3.79, $p_{adj} = 0.0459$; Figure 1b) and MTT reduction assay (DMSO 75.07 ± 4.77 vs. STO-609 63.15 ± 2.70, $p_{adj} = 0.0453$; Figure 1c).

3.2 | CaMKK β knockdown with siRNA exacerbated cell death under OGD with reoxygenation conditions

To confirm the detrimental effect of pharmacological inhibition of CaMKK β during OGD, we used siRNA to knockdown of CaMKK β and investigate its effect in the cell viability in HBEC-5i endothelial cells subjected to 18-hr OGD with 24-hr reoxygenation. Statistical analysis using one-way ANOVA found significant main effects in western blot analysis assay ($F_{2,9} = 8.065$, $p = 0.0098$; Figure 2b), CCK-8 cell viability assays ($F_{3,20} = 149.2$, $p < 0.0001$; Figure 2c) and MTT reduction assay ($F_{3,20} = 37.07$, $p < 0.0001$; Figure 2d). Multiple comparisons post hoc analyses revealed a significant reduction in CaMKK β

protein levels compared to cells treated with CaMKK β scrambled siRNA in Figure 2b (CaMKK β siRNA 0.64 ± 0.08 vs. scrambled siRNA 0.95 ± 0.07, p_{adj} = 0.022). A significant reduction in cell viability was also observed in CaMKK β siRNA-treated cells subjected to 18-hr OGD with 24-hr reoxygenation compared with scrambled siRNA-treated cells in the CCK-8 cell viability assay (CaMKK β siRNA 48.80 ± 3.43 vs. scrambled siRNA 53.56 ± 2.46, p_{adj} = 0.0077; Figure 2c) and MTT reduction assay (CaMKK β siRNA 53.67 ± 3.54 vs. scrambled siRNA 64.19 ± 4.17, p_{adj} = 0.0303; Figure 2d). To confirm the specificity of STO-609 for the inhibition of CaMKK β in this study, we treated cells with CaMKK β siRNA followed by STO-609. Data revealed that CaMKKβ siRNA and STO-609 have no synergistic effect to the suppression of endothelial viability under OGD conditions (CaMKK β siRNA + DMSO vs. CaMKK β siRNA + STO-609, p_{adj} = 0.3141; Figure 2e), confirming the STO-609 is specific for CaMKK β in our study.

3.3 | CaMKK inhibition with STO-609 down-regulated phosphorylated SIRT1 under OGD and OGD with reoxygenation conditions

We examined the downstream mediators of CaMKK in ischemic endothelial cells. SIRT1 is a known vascular protector that is phosphorylated by CaMKK, which increases its stability and activity (Wen et al., 2013). We investigated the potential interaction of CaMKK and SIRT1. HBEC-5i endothelial cells were incubated with 10 μM STO-609, sub-jected to 18-hr OGD or 18-hr OGD with 24-hr reoxygenation conditions and analyzed using western blotting. Incubation with 10 μM STO-609 significantly decreased phosphorylated SIT1 (Ser-27) levels in cells subjected to 18-hr OGD ($F_{3,12}$ = 16.81, p = 0.0001; OGD18 hr DMSO vs. OGD18 hr STO 10 μM, p_{adj} = 0.0459, Figure 3b). Consistently, under 18-hr OGD with 24–hr reoxygenation conditions, treatment with 10 μM STO-609 resulted in down-regulated total SIRT1 (normalized to actin; $F_{3,8}$ = 6.055, p = 0.0187; OGD18 hr + Re24 hr DMSO vs. OGD18 hr + Re24 STO 10 μM, p_{adj} = 0.0482, Figure 3c) and phosphorylated SIRT1 (Ser-27) levels (normalized to actin) in HBEC-5i endothelial cells ($F_{3,8}$ = 8.547, p = 0.0071; OGD18 hr + Re24 hr DMSO vs. OGD18 hr + Re24 hr STO 10 μM, p_{adj} = 0.0335, Figure 3d). We additionally normalized pSIRT1 to total SIRT1. We found that the ratio was reduced by STO-609 after OGD ($F_{3,11}$ = 6.554, p_{adj} = 0.0141; Figure 3e). This is consistent with the fact that phosphorylation of SIRT1 was reduced while the total SIRT1 remained unchanged with STO-609 treatment. Accordingly, no reduction in pSIRT1/ total SIRT1 by STO-609 was seen after OGD with reoxy-genation as both phosphorylation and total were decreased by STO-609 (Figure 3f).

3.4 | SIRT1 mediated CaMKK β activity inhibition-induced cell damage in endothelial cells under OGD with reoxygenation conditions

To confirm that STO-609-induced cell death under OGD with reoxygenation conditions was mediated by SIRT1 activity, we further investigated the viability of endothelial cells treated with STO-609 or/and the pharmacological SIRT1 inhibitor EX-527 and subjected to 18-hr OGD with 24-hr reoxygenation conditions. The CCK-8 cell viability assay revealed that STO-609 treatment significantly reduced cell viability compared with DMSO-treated cells ($F_{4,19}$ = 41.54, p < 0.0001; p_{adj} = 0.0210), and the SIRT1 inhibitor EX-527 increased cell death compared with DMSO treatment (EX-527 44.42 ± 2.89 vs. DMSO 66.50 ± 4.74, p_{adj} = 0.0062; Figure 4a). STO-609 and EX-527 co-treatment also induced significant cell death

compared with DMSO-treated cells (STO-609 + EX-527 45.19 ± 2.09 vs. DMSO 66.50 ± 4.74, $p_{adj} = 0.0071$). However, no difference was observed be-tween EX-527 and STO-609 + EX-527 treatments. Similar results were obtained using the MTT reduction assay. No difference was detected between EX-527 and STO-609 + EX-727 treatments (Figure 4b), which suggests that SIRT1 mediates the effects of CaMKK in endothelial viability under ischemic conditions.

3.5 | Inhibition of CaMKK β by STO-609 regulated CaMKK β and SIRT1 downstream molecules

We further investigated the CaMKK β downstream molecule CaMK IV and SIRT1 downstream molecules, such as eNOS (endothelial nitric oxide synthase), VCAM-1 (vascular cell adhesion molecule 1) and ICAM-1 (intercellular adhesion molecule 1; Wen et al., 2013). Under OGD with reoxygena-tion conditions, as expected, STO-609 reduced the phos-phorylated CaMK IV levels (actin, instead of total CaMK IV, was used as gel loading controls as we did not expect changes in total CaMK IV with STO-609; $F_{3,24} = 38.14$, $p < 0.0001$; DMSO 0.74 ± 0.02 vs. STO-609 0.62 ± 0.03, $p_{adj} = 0.0406$, Figure 5a). STO-609 treatment also decreased eNOS levels ($F_{3,12} = 18.71$, $p < 0.0001$; DMSO 0.85 ± 0.01 vs. STO-609 0.73 ± 0.02, $p_{adj} = 0.0455$, Figure 5b). STO-609 incubation increased VCAM-1 ($F_{3,20} = 105.8$, $p < 0.0001$; DMSO 0.335 ± 0.02 vs. STO-609 0.45 ± 0.03, $p_{adj} = 0.0351$, Figure 5c) and ICAM-1 ($F_{3,16} = 139$, $p < 0.0001$; DMSO 0.62 ± 0.02 vs. STO-609 0.75 ± 0.02, $p_{adj} = 0.0287$, Figure 5d) levels compared with DMSO under OGD with reoxygenation conditions in HBEC-5i endothelial cells.

3.6 | Inhibition of CaMKK exacerbated OGD-induced leukocyte endothelial adhesion

Blood–brain barrier degradation and hemorrhage transforma-tion after ischemic stroke have been associated with the adhe-sion of circulating inflammatory cells, especially neutrophils, to the endothelium and subsequent infiltration into ischemic brain tissue (Rosell et al., 2008; Sun et al., 2014). CaMKK β may exhibit anti-inflammatory effects after OGD with reoxy-genation conditions, which was observed as elevated VCAM-1 and ICAM-1 expression following STO-609 treatment was observed. We performed leukocyte-endothelial adhesion as-says after 18-hr OGD with 24-hr reoxygenation in the presence of DMSO or STO-609 (Figure 6). Optical microscopy images (Figure 6a) revealed that a small number of THP-1 cells bound to the endothelium monolayer under normoxic conditions in cells treated with either DMSO or STO-609. Elevated THP-1 cell adhesion was observed after cells were incubated with DMSO and subjected to OGD with reoxygenation. Interestingly, the number of bound THP-1 cells was higher in STO-609-treated endothelial cells subjected to OGD with reoxygenation than in cells subjected to DMSO treatment. Quantitation of calcein-AM-labeled THP-1 leukocytes to endothelium (Figure 6b) revealed the same results as Figure 6a ($F_{3,16} = 41.72$, $p < 0.0001$; Norm DMSO 100 ± 7.31 vs. OGD + Reox DMSO 157 ± 11.77, $p_{adj} = 0.0020$; OGD + Reox DMSO 157 ± 11.77 vs. OGD + Reox STO 246.25 ± 11.95, $p_{adj} < 0.0001$).

3.7 | CaMKK β activity inhibition exacerbated ischemia-induced BBB leakage in vivo

We further investigated the protective role of CaMKK β on BBB integrity after ischemic stroke using an in vivo model of stroke. The pharmacological inhibitor STO-609 was applied

one hour prior to stroke onset, and Evans blue quantitation was performed to determine cerebrovascular permeability. As shown in Figure 7a, compared to the sham group, mice subjected to MCAO and 24-hr reperfusion treated with vehicle (DMSO) exhibited significantly higher Evans blue extravasation ($F_{2,12} = 37.81$, $p < 0.001$; sham 1.00 ± 0.43 vs. MCAO + DMSO 17.83 ± 6.34, $p_{adj} = 0.05$). Treatment with STO-609 significantly increased the cerebro-vascular permeability compared to mice treated with vehicle (MCAO + DMSO 17.83 ± 6.34 vs. MCAO + STO-609 55.74 ± 8.88, $p_{adj} < 0.001$). Moreover, we performed experi-ments to examine the effect of STO-609 on endothelial cell death using IHC staining and co-localizing cleaved caspase-3 and CD31. CD31 was used to detect brain endothelial cells and cleaved caspase-3 was used to determine apoptosis. As shown in Figure 7b, in the penumbral area, stroke triggered apoptosis in endothelium (MCAO + DMSO) and administration of STO-609 exacerbated the apoptotic cell death in brain endothelial cells after ischemic stroke as more double-staining signal was detected. These data suggest that CaMKK exhibits an intrinsic protective role in the BBB after ischemic stroke.

4 | DISCUSSION

To the best of our knowledge, this study is the first investigation to specifically examine the functional role of CaMKK in endothelial cells and BBB impairment under ischemic conditions. As shown in Figure 8, this study demonstrated the following significant findings. First, we demonstrated that CaMKK inhibition with a pharmacological inhibitor or siRNA increased OGD-induced endothelial cell death. Second, we identified SIRT1 as the key mediator of endothelial CaMKK in ischemic conditions by demonstrating that CaMKK inhibition reduced pSIRT1 levels, and CaMKK inhibition with STO-609 was no longer effective when SIRT1 was pharmacologically inhibited. Third, CaMKK inhibition exacerbated the endothelial production of proinflammatory factors and leukocyte-endothelial adhesion under OGD conditions. Fourth, in an animal model of stroke, ischemia-induced BBB leakage and apoptotic cell death pathway in brain endothelial cells were further aggravated by CaMKK inhibition, which suggests that endogenous CaMKK pro-vides protective effects in BBB integrity during stroke.

Calcium signaling plays critical roles in the pathology of cerebral ischemia. Increased neuronal free calcium activates molecules that participate in signal transduction pathways that lead to cell death (Pivovarova & Andrews, 2010). However, attempts to use calcium blockers failed in ischemic stroke trials (Ginsberg, 2008). It has been increasingly recognized that increased calcium signaling may also play a protective and regenerative role after injury via the triggering of en-dogenous protective pathways. Our laboratory demonstrated that CaMKK, which is a critical upstream kinase involved in calcium signaling, reduced stroke injury. However, the underlying mechanisms were not well studied. Interestingly, deletion of CaMKK increased hemorrhagic transformation in stroke, which suggests that CaMKK influences the BBB and likely EC survival in stroke. The expression of this cascade (CaMKK and CaMK IV) in endothelial cells has been pre-viously reported (Wen et al., 2013). However, no study has specifically examined CaMKK signaling in EC in ischemia. We focused on the role of CaMKK in BBB impairment after stroke with a focus on EC assays. Disruption and malfunction of the blood–brain barrier (BBB) is largely involved in a wide range of neurological disorders, including ischemic stroke

(Saunders, Dziegielewska, Mollgard, & Habgood, 2015; Schoknecht, David, & Heinemann, 2015), which exacerbates injury via several mechanisms, including permeation of peripheral immune cells into the cerebral parenchymal and inducing inflammatory response, which lead to vasogenic edema and hemorrhagic complications (Turner & Sharp, 2016; Zhang et al., 2013). Our present study demonstrated the roles of CaMKK in endothelial survival, endothelial cell-mediated production of factors critical in inflammation, leukocyte infiltration and BBB integrity after ischemia.

We further demonstrated that SIRT1 was the downstream mediator of the effects of CaMKK in EC survival under ischemic conditions. Both CaMKK and its downstream kinase CaMK IV can directly activate SIRT1 (Wen et al., 2013). CaMKK β has been reported to play an important role in the phosphorylation of SIRT1 in endothelial cells during atheroprotective flow. Importantly, SIRT1 phosphorylation by CaMKK at Ser-27 and Ser-47 increases its stability and activity (Wen et al., 2013). Consistently, in our study, we found that incubation with 10 μM STO-609 significantly decreased SIRT1 phosphorylation levels in cells subjected to OGD. Total SIRT1 was also reduced by STO-609 treatment. In a mouse cerebral hypoperfusion model, SIRT1 overexpression exerts vasculoprotection via maintaining unacetylated endothelial nitric oxide synthase (Hattori et al., 2014). In stroke models, SIRT1 activation reduces brain injury (Hernandez-Jimenez et al., 2013). Mice treated with EX527, the SIRT1 inhibitor (Chen et al., 2014), or mice with SIRT1 gene deletion exhibited increased infarcts (Hernandez-Jimenez et al., 2013). In addition, the SIRT1 activator A3 reduced injury in a mouse model of stroke. The mechanisms of this protection are not clear. Very few studies have investigated SIRT1 in cerebral endothelial cells after ischemia. Our work demonstrated that SIRT1 inhibition reduced cell viability, which indicates a protective role for SIRT1 in this cell type after ischemia. However, SIRT1 inhibition in endothelial-astrocytic co-cultures decreased apoptosis and BBB permeability after OGD (Chen et al., 2018). In that study, a mixed culture was used, but the specific effect of SIRT1 inhibition in endothelial cells is not known (Chen et al., 2018). Our work helps establish the role of SIRT1 in endothelial cells and the interaction of CaMKK/SIRT1 in cerebral ischemia.

SIRT1 has been shown to interact with eNOS (Hattori et al., 2014; Mattagajasingh et al., 2007). eNOS-derived NO is essential for endothelial-dependent vasorelaxation and endothelial cell survival (Potente & Dimmeler, 2008). Therefore, eNOS may play a role in the CaMKK/SIRT1-mediated protection in endothelial cells after OGD in our studies. Our data demonstrated decreased levels of eNOS after CaMKK inhibition with STO-609. We found an upregulation of VCAM-1 and ICAM-1 following STO-609 treatment, which are downstream substrates of NO (Wen et al., 2013). VCAM-1 and ICAM-1 are proinflammatory mole-cules that promote inflammatory leukocyte recruitment via signaling cascades involving numerous kinases, including p56lyn. Our leukocyte-endothelial adhesion assay further suggested that VCAM-1 and ICAM-1 are downstream targets of CaMKK. Our work also suggested that CaMKK plays anti-inflammatory roles in ischemia via regulation of leukocyte trafficking. As NO produced by eNOS may produce vasodilatory effects, STO-609 or EX-527 is likely to reduce cerebral blood flow after stroke. Surprising, our previous work showed that STO-609 administration did not alter the degree of cerebral blood flow reduction by MCA occlusion assessed by Laser Doppler Flowmetry (LDF;

McCullough et al., 2013). It is likely STO-609 did not produce significant changes in NO to alter CBF in the in vivo stroke model, challenging the involvement of eNOS in CaMKK mediated effect in an in vivo stroke model. It is also noteworthy LDF measures only a focal point of flow and may not detect subtle changes in cerebral blood flow in the brain. To further investigate potential vasodilation effect of CaMKK in vivo, Laser Speckle may be used to collect more detailed data from larger area of hemispheres and isolated arterial preparation may be utilized ex vivo. We did not assess NO production and the specific vasodilatory effect of CaMKK as the main focus of this project is to define the role CaMKK in EC protection and BBB integrity after stroke. For mechanistic study, the focus of our project is SIRT1. The potential involvement of eNOS and NO in CaMKK mediated EC and brain protection after stroke warrants future investigation.

One limitation of this study is that we only investigated SIRT1 as the direct downstream target of the CaMKK cascade in endothelial cells under ischemic conditions. Evidence suggests that CaMKK also activates AMPK in endothelial cells (Wen et al., 2013), but whether this interaction occurs after OGD is not known. Future studies are warranted for a more comprehensive examination because our work did not exclude other possible targets of CaMKK in ischemic endothelial cells.

In conclusion, using pharmacological and gene knock-down approaches, we demonstrated that CaMKK inhibition in endothelial cells reduced cell viability after OGD. We further identified that SIRT1 mediated the effect of endothelial CaMKK in ischemic conditions. Our data suggest that CaMKK reduces endothelial production of pro-inflammatory factors, leukocyte trafficking and BBB impairment during ischemia. Endothelial CaMKK may be a potential target to reduce injury in ischemic stroke and other cerebrovascular diseases in which BBB impairment plays a role.

ACKNOWLEDGEMENTS

This project was generously supported by National Institutes of Health grants R01 NS099628 (J.Li) and R01 NS078446 (J.Li).

Funding information

National Institute of Neurological Disorders and Stroke, Grant/Award Number: R01 NS078446 and R01 NS099628

Abbreviations:

BBB	blood–brain barrier
CaMKK	calcium/calmodulin-dependent protein kinase kinase
DMSO	dimethylsulfoxide
EC	endothelial cells
eNOS	endothelial nitric oxide synthase
HBEC	human brain microvascular endothelial cells
ICAM-1	intercellular adhesion molecule-1

MCAO	middle cerebral artery occlusion
OGD	oxygen-glucose deprivation
SIRT1	sirtuin 1
VCAM-1	vascular cell adhesion molecule-1

REFERENCES

Chen T, Dai SH, Li X, Luo P, Zhu J, Wang YH, … Jiang XF (2018). Sirt1-Sirt3 axis regulates human blood–brain barrier permeability in response to ischemia. Redox Biology, 14, 229–236. 10.1016/j.redox.2017.09.016 [PubMed: 28965081]

Chen HZ, Guo S, Li ZZ, Lu Y, Jiang DS, Zhang R, … Li H (2014). A critical role for interferon regulatory factor 9 in cerebral ischemic stroke. Journal of Neuroscience, 34, 11897–11912. 10.1523/JNEUROSCI.1545-14.2014 [PubMed: 25186738]

Ginsberg MD (2008). Neuroprotection for ischemic stroke: Past, present and future. Neuropharmacology, 55, 363–389. 10.1016/j.neuropharm.2007.12.007 [PubMed: 18308347]

Hattori Y, Okamoto Y, Maki T, Yamamoto Y, Oishi N, Yamahara K, … Ihara M (2014). Silent information regulator 2 homolog 1 counters cerebral hypoperfusion injury by deacetylating endothelial nitric oxide synthase. Stroke, 45, 3403–3411. 10.1161/STROKEAHA.114.006265 [PubMed: 25213338]

Hernandez-Jimenez M, Hurtado O, Cuartero MI, Ballesteros I, Moraga A, Pradillo JM, … Moro MA (2013). Silent information regulator 1 protects the brain against cerebral ischemic damage. Stroke, 44, 2333–2337. 10.1161/STROKEAHA.113.001715 [PubMed: 23723308]

Liu L, Doran S, Xu Y, Manwani B, Ritzel R, Benashski S, … Li J (2014). Inhibition of mitogen-activated protein kinase phosphatase-1 (MKP-1) increases experimental stroke injury. Experimental Neurology, 261, 404–411. 10.1016/j.expneurol.2014.05.009 [PubMed: 24842488]

Liu L, Yuan H, Denton K, Li XJ, McCullough L, & Li J (2016). Calcium/calmodulin-dependent protein kinase kinase beta is neuro-protective in stroke in aged mice. European Journal of Neuroscience, 44, 2139–2146. 10.1111/ejn.13299 [PubMed: 27305894]

Manaenko A, Chen H, Kammer J, Zhang JH, & Tang J (2011). Comparison Evans Blue injection routes: Intravenous versus intraperitoneal, for measurement of blood–brain barrier in a mice hemorrhage model. Journal of Neuroscience Methods, 195, 206–210. 10.1016/j.jneumeth.2010.12.013 [PubMed: 21168441]

Mattagajasingh I, Kim CS, Naqvi A, Yamamori T, Hoffman TA, Jung SB, … Irani K (2007). SIRT1 promotes endothelium-dependent vascular relaxation by activating endothelial nitric oxide synthase. Proceedings of the National Academy of Sciences of the United States of America, 104, 14855–14860. 10.1073/pnas.0704329104 [PubMed: 17785417]

McCullough LD, Tarabishy S, Liu L, Benashski S, Xu Y, Ribar T, … Li J (2013). Inhibition of calcium/calmodulin-dependent protein kinase kinase beta and calcium/calmodulin-dependent protein kinase IV is detrimental in cerebral ischemia. Stroke, 44, 2559–2566. 10.1161/STROKEAHA.113.001030 [PubMed: 23868268]

Okada Y, & Okada M (2013). Protective effects of plant seed extracts against amyloid beta-induced neurotoxicity in cultured hippocampal neurons. Journal of Pharmacy and Bioallied Sciences, 5, 141–147. 10.4103/0975-7406.111819 [PubMed: 23833520]

Pan Q, He C, Liu H, Liao X, Dai B, Chen Y, … Ma X (2016). Microvascular endothelial cells-derived microvesicles imply in ischemic stroke by modulating astrocyte and blood brain barrier function and cerebral blood flow. Molecular Brain, 9, 63 10.1186/s13041-016-0243-1 [PubMed: 27267759]

Pivovarova NB, & Andrews SB (2010). Calcium-dependent mito-chondrial function and dysfunction in neurons. FEBS Journal, 277, 3622–3636. 10.1111/j.1742-4658.2010.07754.x [PubMed: 20659161]

Plumb JA, Milroy R, & Kaye SB (1989). Effects of the pH dependence of 3-(4,5-dimethylthiazol-2-yl)-2,5-diphenyl-tetrazolium bromide-formazan absorption on chemosensitivity determined by a novel tetrazolium-based assay. Cancer Research, 49, 4435–4440. [PubMed: 2743332]

Potente M, & Dimmeler S (2008). Emerging roles of SIRT1 in vascu-lar endothelial homeostasis. Cell Cycle, 7, 2117–2122. 10.4161/cc.7.14.6267 [PubMed: 18641460]

Rosell A, Cuadrado E, Ortega-Aznar A, Hernandez-Guillamon M, Lo EH, & Montaner J (2008). MMP-9-positive neutrophil in-filtration is associated to blood–brain barrier breakdown and basal lamina type IV collagen degradation during hemorrhagic transfor-mation after human ischemic stroke. Stroke, 39, 1121–1126. 10.1161/STROKEAHA.107.500868 [PubMed: 18323498]

Sandoval KE, & Witt KA (2008). Blood–brain barrier tight junction permeability and ischemic stroke. Neurobiology of Diseases, 32, 200–219. 10.1016/j.nbd.2008.08.005

Saunders NR, Dziegielewska KM, Mollgard K, & Habgood MD (2015). Markers for blood–brain barrier integrity: How appropri-ate is Evans blue in the twenty-first century and what are the alternatives? Frontiers in Neuroscience, 9, 385. [PubMed: 26578854]

Schoknecht K, David Y, & Heinemann U (2015). The blood–brain barrier-gatekeeper to neuronal homeostasis: Clinical implications in the setting of stroke. Seminars in Cell & Developmental Biology, 38, 35–42. 10.1016/j.semcdb.2014.10.004 [PubMed: 25444848]

Sun P, Esteban G, Inokuchi T, Marco-Contelles J, Weksler BB, Romero IA, … Sole M (2015). Protective effect of the multitar-get compound DPH-4 on human SSAO/VAP-1-expressing hCMEC/D3 cells under oxygen-glucose deprivation conditions: An in vitro experimental model of cerebral ischaemia. British Journal of Pharmacology, 172, 5390–5402. 10.1111/bph.13328 [PubMed: 26362823]

Sun P, Hernandez-Guillamon M, Campos-Martorell M, Simats A, Montaner J, Unzeta M, & Sole M (2018). Simvastatin blocks soluble SSAO/VAP-1 release in experimental models of cerebral ischemia: Possible benefits for stroke-induced inflammation con-trol. Biochimica et Biophysica Acta, 1864, 542–553. 10.1016/j.bbadis.2017.11.014 [PubMed: 29175057]

Sun P, Sole M, & Unzeta M (2014). Involvement of SSAO/VAP-1 in oxygen-glucose deprivation-mediated damage using the endothe-lial hSSAO/VAP-1-expressing cells as experimental model of cere-bral ischemia. Cerebrovascular Disease, 37, 171–180. 10.1159/000357660

Turner RJ, & Sharp FR (2016). Implications of MMP9 for blood brain barrier disruption and hemorrhagic transformation following ischemic stroke. Frontiers in Cellular Neuroscience, 10, 56. [PubMed: 26973468]

Wen L, Chen Z, Zhang F, Cui X, Sun W, Geary GG, … Shyy JY (2013). Ca2+/calmodulin-dependent protein kinase kinase beta phosphorylation of sirtuin 1 in endothelium is atheroprotective. Proceedings of the National Academy of Sciences of the United States of America, 110, E2420–E2427. 10.1073/pnas.1309354110 [PubMed: 23754392]

Yin KJ, Deng Z, Hamblin M, Xiang Y, Huang H, Zhang J, … Chen YE (2010). Peroxisome proliferator-activated receptor delta regulation of miR-15a in ischemiainduced cerebral vascular endothelial injury. Journal of Neuroscience, 30, 6398–6408. 10.1523/JNEUROSCI.0780-10.2010 [PubMed: 20445066]

Yin KJ, Fan Y, Hamblin M, Zhang J, Zhu T, Li S, … Chen YE (2013). KLF11 mediates PPARgamma cerebrovascular protection in ischaemic stroke. Brain, 136, 1274–1287. 10.1093/brain/awt002 [PubMed: 23408111]

Yuan H, Denton K, Liu L, Li XJ, Benashski S, McCullough L, & Li J (2016). Nuclear translocation of histone deacetylase 4 induces neuronal death in stroke. Neurobiology of Diseases, 91, 182–193. 10.1016/j.nbd.2016.03.004

Zhang Y, Zhang P, Shen X, Tian S, Wu Y, Zhu Y, … Hu Y (2013). Early exercise protects the blood–brain barrier from ischemic brain injury via the regulation of MMP-9 and occludin in rats. International Journal of Molecular Sciences, 14, 11096–11112. 10.3390/ijms140611096 [PubMed: 23708107]

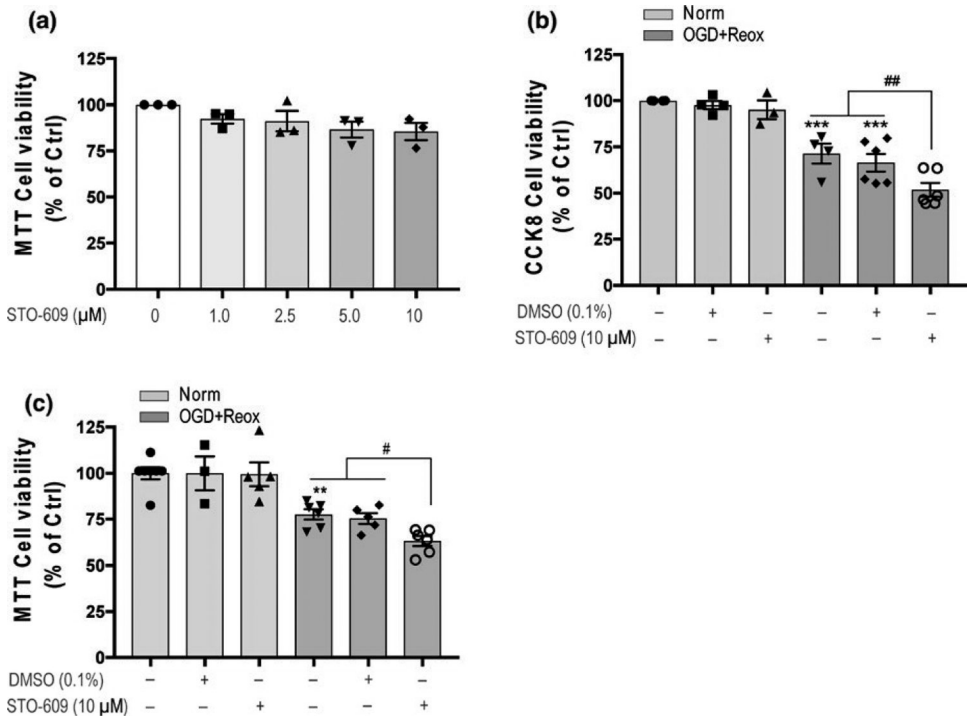

FIGURE 1.

CaMKK β activity inhibition by STO-609 induced cell death of human brain microvascular endothelial cells (HBEC-5i) under OGD conditions. (a) Influence of CaMKK β inhibitor STO-609 (1.0–10 μM) on cell viability under normoxic conditions for 24 hr. Cells without STO-609 treatment were considered control cells. MTT reduction assay was used to assess cell viability; (b) and (c) The inhibition of CaMKK β activity with STO-609 under 18-hr OGD with 24 hr of reoxygenation (OGD + Reox) reduced cell viability in HBEC-5i cells in the CCK-8 cell proliferation assay and MTT reduction assay. STO-609 (10 μM) was added prior to OGD and maintained during reoxygenation. Control cells were non-treated cells in normoxic conditions (Norm). Data are expressed as the means ± *SEM* of at least three independent experiments. *$p < 0.05$, **$p < 0.01$ and ***$p < 0.001$ versus non-treated cells under normoxia. $^{\#}p < 0.05$ between the indicated treatments. Statistical analyses were performed using one-way ANOVA and the Holm-Sidak multiple comparison test

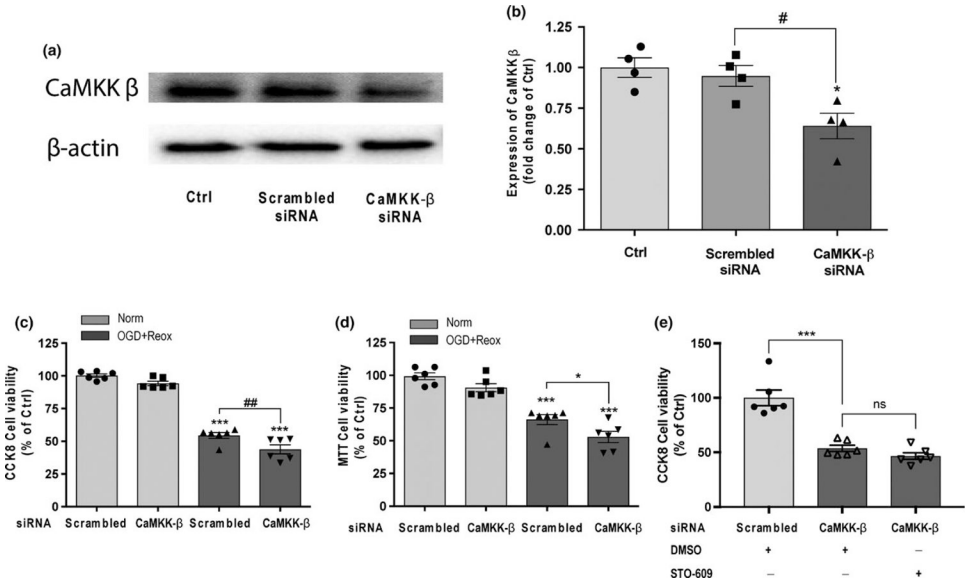

FIGURE 2.

Knockdown of CaMKK β expression exacerbated cell death under OGD with reoxygenation conditions in HBEC-5i endothelial cells. (a) and (b) Representative western blot images and quantitation of CaMKK β expression in HBEC-5i treated with scrambled siRNA and CaMKK β siRNA for 2 hr under normoxic conditions. Cells without siRNA treatment were considered control cells (Ctrl). Quantitation of CaMKK β was normalized to β-actin levels. (c) and (d) CaMKK β knock down using siRNA reduced cell viability in HBEC-5i cells under 18-hr OGD with 24 hr of reoxygenation (OGD + Reox) in the CCK-8 cell proliferation assay and MTT reduction assay. Scrambled siRNA (60 nM) and CaMKK β siRNA (60 nM) were incubated with the cells for 7 hr, normal growth medium containing 2× normal serum and antibiotic concentration was added and incubated for 24 hr. Cells were replaced with fresh 1× normal growth medium for another 24 hr of recovery prior to OGD and reoxygenation treatments. (e) STO-609 and CaMKK β had no additive effect in cell viability after OGD using CCK-8 cell assay. CaMKK β siRNA and STO-609 (10 μM) were added prior to OGD (18 hr) and maintained during reoxygenation (24 hr). Cells treated with scrambled siRNA under normoxic conditions (Norm) were considered control cells (Ctrl). Data are expressed as the means ± *SEM* of at least four independent experiments. $*p < 0.05$ and $***p < 0.001$ versus Ctrl in the corresponding experiment. $^{\#}p < 0.05$ and $^{\#\#}p < 0.01$ between the indicated treatments. Statistical analyses were performed using one-way ANOVA and the Holm-Sidak multiple comparison test

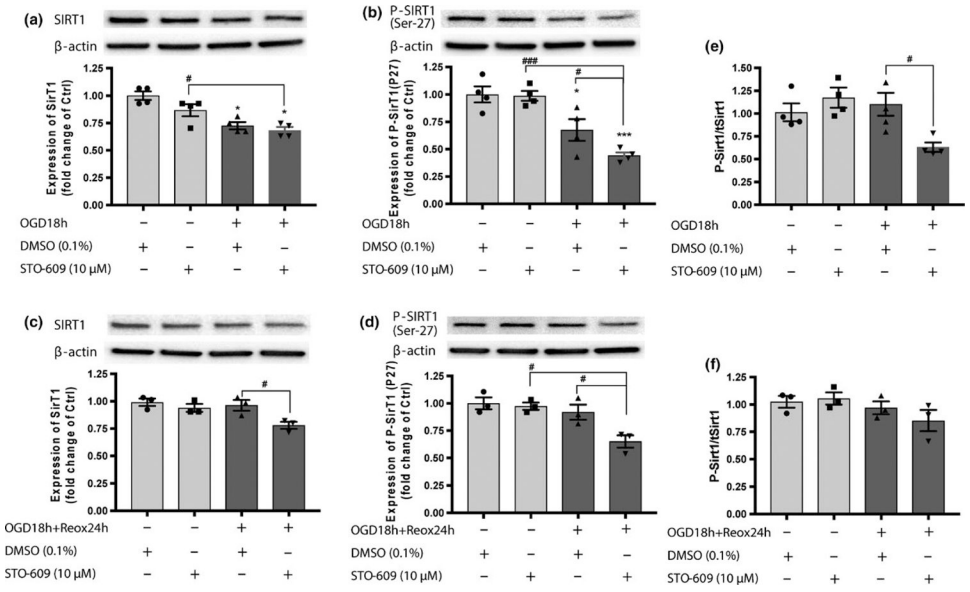

FIGURE 3.

Inhibition CaMKK β activity with STO-609 down-regulated SIRT1 phosphorylation under OGD and OGD with reoxygenation conditions in HBEC-5i endothelial cells. (a) and (b) Representative western blot images and quantitation of SIRT1 and phosphorylated SIRT1 (P-SIRT1, Ser-27) expression in HBEC-5i cells treated with DMSO (0.1%) or STO-609 (10 μM) under normoxia or 18-hr OGD. (c) and (d) Representative Western blot images and quantitated data analysis of SIRT1 and phosphorylated SIRT1 (P-SIRT1, Ser-27) expression in HBEC-5i cells treated with DMSO (0.1%) or STO-609 (10 μM) under normoxia or 18-hr OGD with 24 hr of reoxygenation (OGD18 hr + Reox24 hr). Quantitation of SIRT1 or P-SIRT1 was normalized to β-actin levels. Cells treated with DMSO and without OGD treatments were considered control cells (Ctrl). (e) and (f) Normalized pSIRT1 to total SIRT1 ratio under OGD18 hr or OGD18 hr + Reox24 hr. Data are expressed as the means ± *SEM* of at least three independent experiments. $*p < 0.05$, $**p < 0.01$ and $***p < 0.001$ versus DMSO-treated cells under normoxic conditions. $^{\#}p < 0.05$ and $^{\#\#\#}p < 0.001$ STO-609-treated cells under OGD or OGD with reoxygenation conditions. Statistical analyses were performed using one-way ANOVA and the Holm-Sidak multiple comparison test

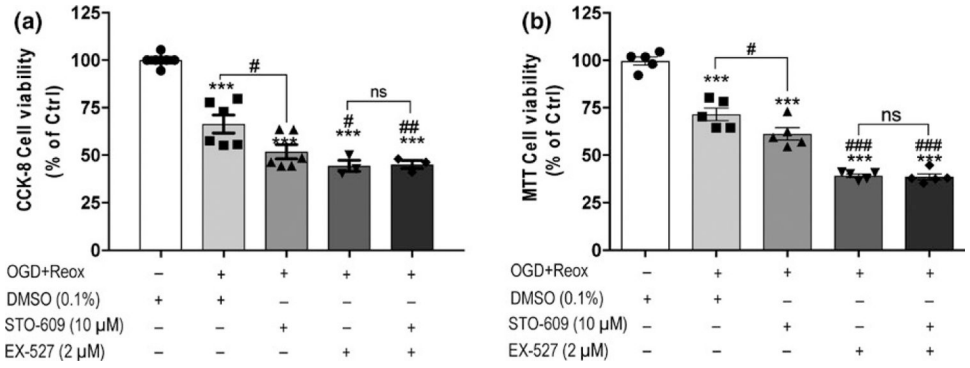

FIGURE 4.

SIRT1 mediated STO-609-induced cell death of HBEC-5i endothelial cells under OGD with reoxygenation conditions. (a) The inhibitory effect of CaMKK activity by STO-609, the inhibitory effect of SIRT1 activity by the SIRT1 inhibitor EX-527, and co-treatment of STO-609 and EX-527 on the viability of HBEC-5i cells under 18-hr OGD with 24-hr reoxygenation (OGD + Reox) were detected using the CCK-8 cell proliferation assay. (b) MTT reduction assay was performed to assess cell viability under the same conditions as (a). DMSO (0.1%), STO-609 (10 μM) and EX-527 (2 μM) were added prior to OGD and maintained during reoxygenation. Cells treated with DMSO (0.1%) under normoxic conditions were considered control cells (Ctrl). Data are expressed as the means ± *SEM* of at least three independent experiments. ***$p < 0.001$ versus control cells. $^{\#\#}p < 0.01$ and $^{\#\#\#}p < 0.001$ versus DMSO-treated cells under OGD + Reox conditions. Not significant (ns) between indicated treatments. Statistical analyses were performed using one-way ANOVA and the Holm-Sidak multiple comparison test

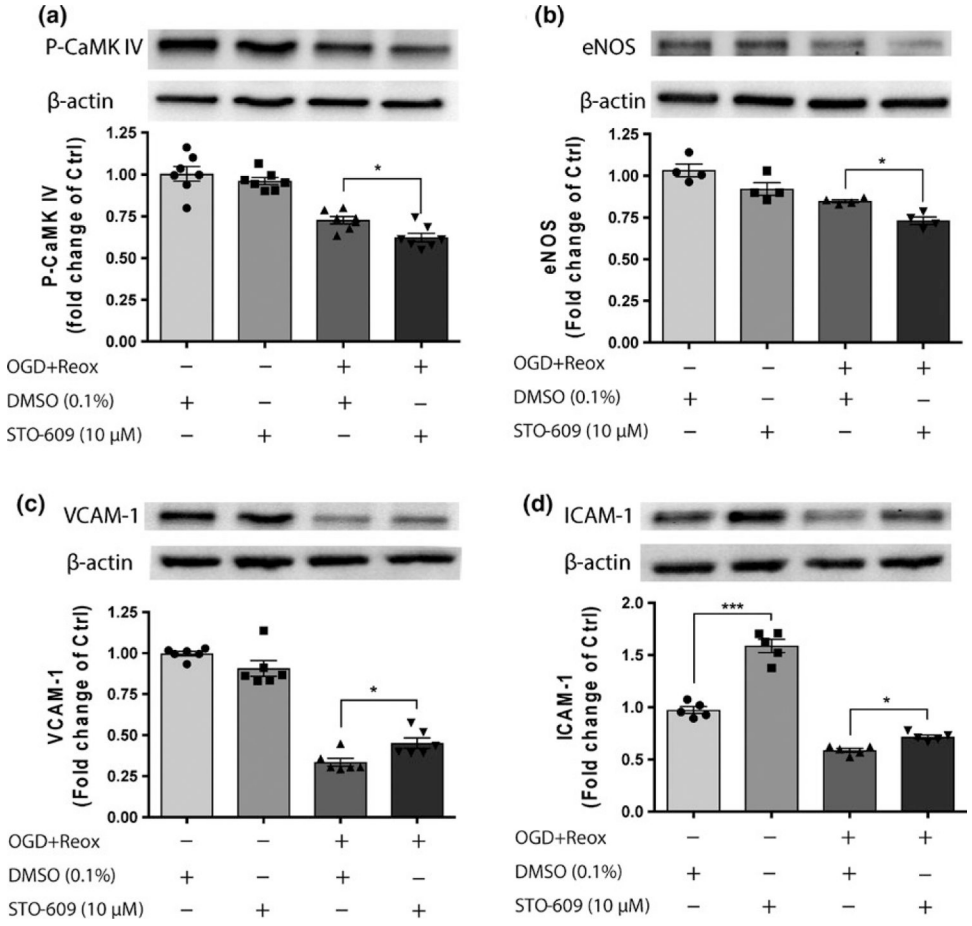

FIGURE 5.

Effects of STO-609 on CaMKK/SIRT1 down-stream molecules after OGD in HBEC-5i endothelial cells. Representative western blot images and quantitation of the CaMKK β down-stream molecule phosphorylated CaMK IV (P-CaMK IV) (a), SIRT1 downstream molecules, e-NOS (b), VCAM-1 (c) and ICAM-1 (d) expression in HBEC-5i endothelial cells subjected to 18-hr OGD with 24-hr reoxygenation (OGD + Reox) in the presence of DMSO (0.1%) or STO-609 (10 μM). The level of each protein was normalized to β-actin levels. DMSO-treated cells under normoxic conditions were considered control samples (Ctrl). Data are expressed as the means ± *SEM* of at least four independent experiments. *$p < 0.05$ and ***$p < 0.001$ between the indicated treatments. Statistical analyses were performed using one-way ANOVA and the Holm-Sidak multiple comparison test

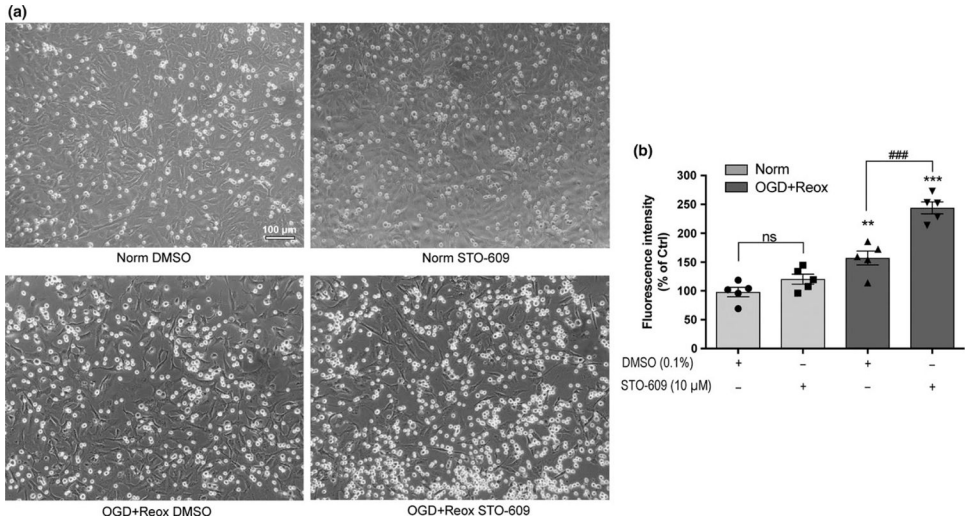

FIGURE 6.

Inhibition of CaMKK β activity increased leukocyte adhesion to endothelial cells under OGD with reoxygenation conditions. The leukocyte-endothelium adhesion assay was performed to analyze the anti-inflammatory effects mediated by CaMKK β activity. (a) Representative optical microscopy images of HBEC-5i endothelial cell monolayers and binding leukocytes (THP-1 cells) treated with DMSO (0.1%) or STO-609 (10 μM) under normoxic conditions (Norm) or 18-hr OGD with 24-hr reoxygenation (OGD + Reox). (b) Fluorescence intensity of the bound calcein-AM labeled leukocytes was quantitated after the same treatments as (a). DMSO-treated cells under normoxic conditions were considered control (Ctrl). Data are expressed as the means ± *SEM* of five independent experiments. $^{**}p < 0.01$, $^{***}p < 0.001$ versus control cells. $^{\#\#\#}p < 0.001$ versus DMSO-treated cells under OGD + Reox conditions. Not significant (ns) between indicated treatments. Statistical analyses were performedusing one-way ANOVA and the Holm-Sidak multiple comparison test. [Colour figure can be viewed at wileyonlinelibrary.com]

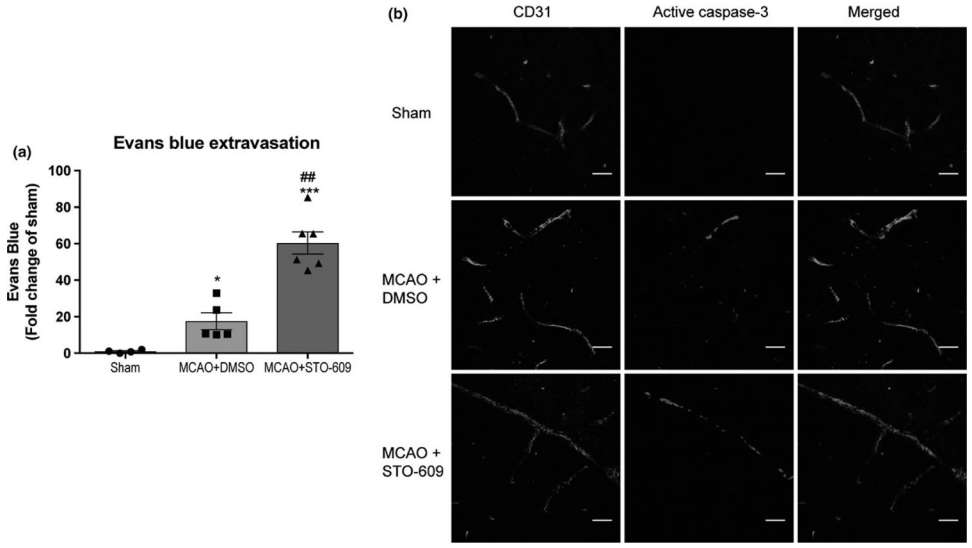

FIGURE 7.

CaMKK β inhibition by STO-609 increases cerebrovascular permeability and endothelial cell apoptosis in vivo. (a) Evans blue extravasation was carried out to evaluate the cerebrovascular permeability. (b) STO-609 treatment exacerbated endothelial cell apoptosis in the penumbra 24 hr after MCAO. CD31 positive signal was shown in green color and cleaved caspase-3 was shown in red color. Scale bar: 20 μM. Mice were treated with DMSO or STO-609 1-hr before 90 min of middle cerebral artery occlusion (MCAO) and brains were harvested 24 hr after MCAO. BBB permeability data are expressed as mean ± *SEM* (n = 4 for sham group, n = 5 for MCAO + DMSO group and n = 6 for MCAO + STO-609 group). *$p < 0.05$, ***$p < 0.001$ versus sham group. $^{\#\#}p < 0.05$ versus MCAO + DMSO group. Statistical analyses were performed by one-way ANOVA tests followed by Holm-Sidak multiple comparison test. [Colour figure can be viewed at wileyonlinelibrary.com]

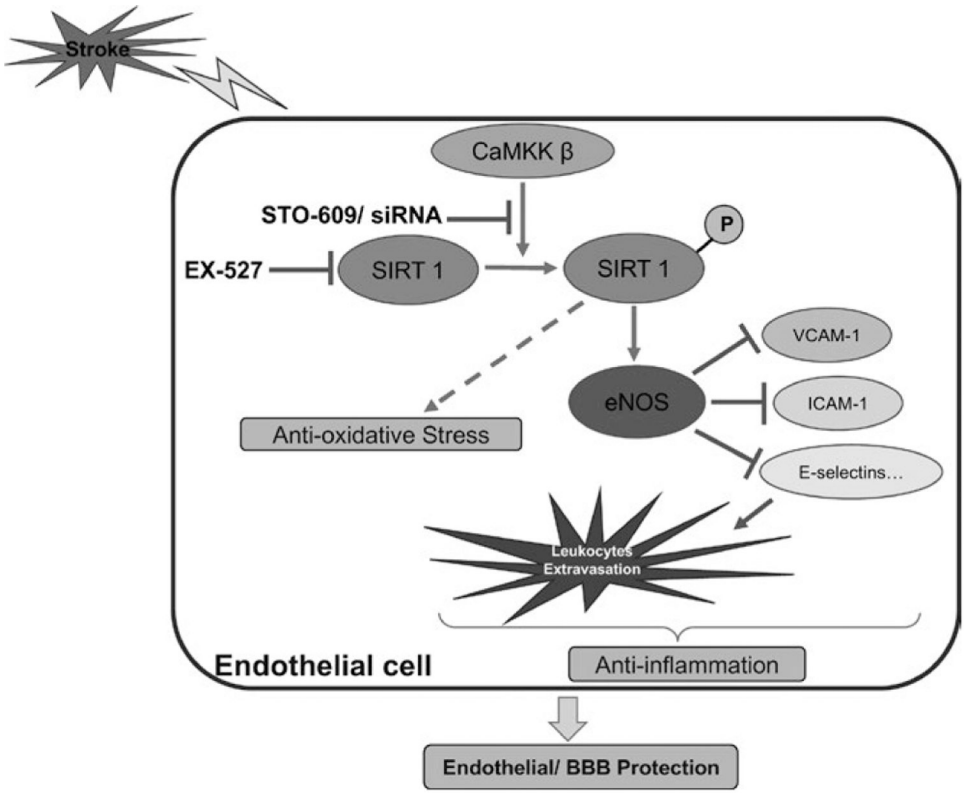

FIGURE 8.

Graphic summary of protective roles potential mechanisms of CaMKK in endothelial cells and BBB under ischemic conditions. In brain endothelial cells after stroke, CaMKK β activates SIRT1 by phosphorylation, which subsequently produces anti-oxidative effect and enhances eNOS signaling. eNOS signaling then produces pleiotropic effects including endothelial cell protection and inhibiting inflammation by reducing VCAM-1, ICAM-1, E-selectins and leukocytes extravasation. STO-609 and EX-527 are pharmacological inhibitors of CaMKK and SIRT1, respectively. BBB: blood–brain barrier; CaMKK β: Calcium/ Calmodulin-Dependent Protein Kinase Kinase β; eNOS: endothelial nitric oxide synthase; ICAM-1: intercellular adhesion molecule −1; SIRT1: sirtuin 1; VCAM-1: vascular cell adhesion molecule-1. [Colour figure can be viewed at wileyonlinelibrary.com]